

The effect of forbidden transitions on cosmological hydrogen and helium recombination

Wan Yan Wong* and Douglas Scott†

Department of Physics and Astronomy, University of British Columbia, 6224 Agricultural Rd., Vancouver, BC, V6T 1Z1, Canada

2006 December

ABSTRACT

More than half of the atoms in the Universe recombined via forbidden transitions, so that accurate treatment of the forbidden channels is important in order to follow the cosmological recombination process with the level of precision required by future microwave anisotropy experiments. We perform a multi-level calculation of the recombination of hydrogen (H) and helium (He) with the addition of the $2^3P_1-1^1S_0$ spin-forbidden transition for neutral helium (He I), plus the $nS-1S$ and $nD-1S$ two-photon transitions for H (up to $n = 40$) and among singlet states of He I ($n \leq 10$ and $\ell \leq 7$). The potential importance of such transitions was first proposed by Dubrovich & Grachev (2005) using an effective three-level atom model. Here, we relax the thermal equilibrium assumption among the higher excited states to investigate the effect of these extra forbidden transitions on the ionization fraction x_e and the Cosmic Microwave Background (CMB) angular power spectrum C_ℓ . The spin-forbidden transition brings more than a percent change in x_e . The two-photon transitions may also give non-negligible effects, but currently accurate rates exist only for $n \leq 3$. We find that changes in both x_e and C_ℓ would be at about the percent level with the approximate rates given by Dubrovich & Grachev (2005). However, the two-photon rates from $3S$ to $1S$ and $3D$ to $1S$ of H appear to have been overestimated, and our best numerical calculation puts the effect on x_e and C_ℓ at below the percent level. Nevertheless, we do not claim that we have the definite answer, since several issues remain open; sub-percent level computation of the C_ℓ s requires improved calculations of atomic transition rates as well as increasingly complex multi-level atom calculations.

Key words: cosmology: cosmic microwave background – cosmology: early universe – cosmology: theory – atomic processes.

1 INTRODUCTION

The release of the third year data from the Wilkinson Microwave Anisotropy Probe (WMAP) has further improved the precision with which we can constrain the cosmological parameters from the shape of the Cosmic Microwave Background (CMB) anisotropies C_ℓ (Spergel et al. 2006). The *Planck* satellite, scheduled for launch in 2008 (Planck 2006), will provide even higher precision C_ℓ values and data down to smaller angular scales ($\ell \lesssim 2500$). Higher precision in the observations requires increased accuracy from the theoretical calculations, in order for the correct cosmological parameters to be extracted. It now seems crucial to obtain the C_ℓ s down to at least the 1 percent level over a wide range of ℓ .

CMBFAST (Seljak & Zaldarriaga 1996) is the most commonly used Boltzmann code for calculating the C_ℓ s, and it gives consistent results with other independent codes (see Seljak et al. 2003, and references therein). The dominant uncertainty in obtaining accurate C_ℓ s comes from details in the physics of recombination, for example, the ‘fudge factor’ in the RECFAST routine (Seager, Sasselov & Scott 1999, 2000). Calculations of cosmological recombination were first published by Peebles (1968) and Zel’dovich, Kurt & Sunyaev (1968). Seager, Sasselov & Scott (2000) presented the most detailed multi-level calculation and introduced a fudge factor to reproduce the results within an effective three-level model. Although the multi-level calculation already gives reasonable accuracy, the required level of accuracy continues to increase, so that today any effect which is ~ 1 per cent over a range of multipoles is potentially significant. Several modifications have been recently suggested to give per cent level changes in the ionization fraction and/or the C_ℓ s (see Section 4 for details). Most of these modifications have been

* E-mail: wanyan@phas.ubc.ca

† E-mail: dscott@phas.ubc.ca

calculated only with an effective three-level code, and so the results may be different in the multi-level calculation, since there is no thermal equilibrium assumed between the upper states. Here we want to focus on one of these modifications, namely the extra forbidden transitions proposed by Dubrovich & Grachev (2005), which we study using a multi-level code.

In the standard calculations of recombination, one considers all the resonant transitions, but only one forbidden transition, which is the 2S–1S two-photon transition, and this can be included for both H and He. Dubrovich & Grachev (2005) suggested that one should also include the two-photon transitions from higher excited S and D states to the ground state for H and HeI, and also the spin-forbidden transition between the triplet 2^3P_1 and singlet ground state 1^1S_0 for HeI. They showed that the recombination of both H and HeI sped up in the three-level atom model. The suggested level of change is large enough to bias the determination of the cosmological parameters (Lewis, Weller & Battye 2006).

The purpose of this paper is to investigate the effect of the extra forbidden transitions suggested by Dubrovich & Grachev (2005) in the multi-level atom model without assuming thermal equilibrium among the higher excited states. The outline of the paper is as follows. In Section 2 we will describe details of the rate equations in our numerical model. In Section 3 we will present results on the ionization fraction x_e and the anisotropies C_ℓ , and assess the importance of the addition of the forbidden transitions. Other possible improvements of the recombination calculation will be discussed in Section 4. And finally in Section 5 we will present our conclusions.

2 MODEL

In this paper we follow the formalism of the multi-level calculation performed by Seager, Sasselov & Scott (2000). We consider 100 levels for HI, 103 levels for HeI, 10 levels for HeII, 1 level for HeIII, 1 level for the electrons and 1 level for the protons. For H, we only consider discrete n levels and assume that the angular sub-levels (ℓ -states) are in statistical equilibrium within a given shell. For both HeI and HeII, we consider all the ℓ -states separately. The multilevel HeI atom includes all states with $n \leq 10$ and $\ell \leq 7$. Here we give a summary of the rate equations for the number density of each energy level i , and the equation for the change of matter temperature T_M . The rate equation for each state with respect to redshift z is

$$(1+z) \frac{dn_i}{dz} = -\frac{1}{H(z)} \times \left[(n_e n_c R_{ci} - n_i R_{ic}) + \sum_{j=1}^N \Delta R_{ji} \right] + 3n_i, \quad (1)$$

where n_i is the number density of the i th excited atomic state, n_e is the number density of electrons, and n_c is the number density of continuum particles such as a proton, HeII, or HeIII ion. Additionally R_{ci} is the photo-recombination rate, R_{ic} is the photo-ionization rate, ΔR_{ji} is the net bound-bound rate for each line transition, and $H(z)$ is the Hubble parameter. We do not include the

collisional rates, as they have been shown to be negligible (Seager, Sasselov & Scott 2000).

For HeI, we update the atomic data for the energy levels (Morton, Wu & Drake 2006), the oscillator strength for resonant transitions (Drake & Morton, in preparation) and the photo-ionization cross-section spectrum. We use the photo-ionization cross-section given by Hummer & Storey (1998) for $n \leq 10$ and $\ell \leq 4$, and adopt the hydrogenic approximation for states with $\ell \geq 5$ (Storey & Hummer 1991). It is hard to find published accurate and complete data for the photo-ionization cross-section of HeI with large n and ℓ . For example, a recent paper by Bauman et al. (2005) claimed that they had calculated the photo-ionization cross-section up to $n = 27$ and $\ell = 26$, although, no numerical values were provided.

The rate of change of matter temperature with respect to redshift is

$$(1+z) \frac{dT_M}{dz} = \frac{8\sigma_T U}{3H(z)m_e c} \frac{n_e}{n_e + n_H + n_{He}} (T_M - T_R) + 2T_M, \quad (2)$$

where T_R is the radiation temperature, n_{He} is the total number density for helium, m_e is the electron mass, c is the speed of light, $U = a_R T_R^4$, a_R is the radiation constant and σ_T is the Thompson scattering cross-section.

Seager, Sasselov & Scott (2000) considered all the resonant transitions and only one forbidden transition, namely the 2S–1S two-photon transition, in the calculation of each atom, (for HeI, $2S \equiv 2^1S_0$ and $1S \equiv 1^1S_0$). The 2S–1S two-photon transition rate is given by

$$\Delta R_{2S \rightarrow 1S} = \Lambda_{2S} \left(n_{2S} - n_{1S} \frac{g_{2S}}{g_{1S}} e^{-h_P \nu_{2S-1S}/k_B T_M} \right), \quad (3)$$

where Λ_{2S} is the spontaneous rate of the corresponding two-photon transition, ν_{2S-1S} is the frequency between levels 2S and 1S, g_i is the degeneracy of the energy level i , h_P is Planck's constant and k_B is Boltzmann's constant.

Here we include the following extra forbidden transitions, which were first suggested by Dubrovich & Grachev (2005). The first ones are the two-photon transitions from nS and nD to $1S$ for H, plus n^1S_0 and n^1D_2 to 1^1S_0 for HeI. For example, for H, we can group together the nS and nD states coming from the same level, so that we can write the two-photon transition rate as

$$\Delta R_{nS+nD \rightarrow 1S}^H = \Lambda_{nS+nD}^H \times \left(n_{nS+nD} - n_{1S} \frac{g_{nS+nD}}{g_{1S}} e^{-h_P \nu_{n1}/k_B T_M} \right). \quad (4)$$

Here n (without a subscript) is the principle quantum number of the state, n_{nS+nD} is the total number density of the excited atoms in either the nS or nD states, and Λ_{nS+nD}^H is the effective spontaneous rate of the two-photon transition from $nS+nD$ to $1S$, which is approximated by the following formula (Dubrovich & Grachev 2005):

$$\Lambda_{nS+nD}^H = \frac{54\Lambda_{2S}^H}{g_{nS+nD}} \left(\frac{n-1}{n+1} \right)^{2n} \frac{11n^2 - 41}{n}, \quad (5)$$

where Λ_{2S}^H is equal to 8.2290 s^{-1} (Goldman 1989; Santos, Parente & Indelicato 1998). The latest value of Λ_{2S}^H is equal to 8.2206 s^{-1} (Labzowsky, Shonin & Solov'yev 2005) and does not bring any noticeable change to the result. Here g_{nS+nD} is equal to 1 for $n=2$, and 6 for $n \geq 3$. This

spontaneous rate is estimated by considering only the non-resonant two-photon transitions through one intermediate state nP . Dubrovich & Grachev (2005) ignored the resonant two-photon transition contributions, since the escape probability of these emitted photons is very low. The above formula for Λ_{nS+nD}^H is valid up to $n \simeq 40$, due to the dipole approximation used, although it is not trivial to check how good this approximate rate is. Besides the 2S–1S two-photon rate, only the non-resonant two-photon rates from 3S to 1S and 3D to 1S are calculated accurately and available in the literature. Cresser et al. (1986) evaluated Λ_{3S}^H and Λ_{3D}^H by including the non-resonant transitions through the higher-lying intermediate nP states ($n \geq 4$), which are equal to 8.2197 s^{-1} and 0.13171 s^{-1} , respectively. These values were confirmed by Florescu, Schneider & Mihailescu (1988) and agreed to three significant figures. Using these values, we find that Λ_{nS+nD}^H is equal to 1.484 s^{-1} , which is an order of magnitude smaller than the value from the approximated rate coming from equation (5). The approximation given by Dubrovich & Grachev (2005) therefore seems to be an overestimate. This leads us instead to consider a scaled rate $\tilde{\Lambda}_{nS+nD}^H$, which is equal to Λ_{nS+nD}^H multiplied by a factor to bring the approximated two-photon rates of H (equation (5)) with $n=3$ into agreement with the numerical value given above, i.e.

$$\tilde{\Lambda}_{nS+nD}^H = 0.0664 \Lambda_{nS+nD}^H. \quad (6)$$

Note that the use of the non-resonant rates is an approximation. The resonant contributions are suppressed in practice because of optical depth effects, and in a sense some of these contributions are already included in our multi-level calculation. Nevertheless, the correct way to treat these effects would be in a full radiative transfer calculation, which we leave for a future study. For HeI, we treat n^1S_0 and n^1D_2 separately and use equation (3) for calculating the transition rates. The spontaneous rate $\Lambda_{nS/nD}^{\text{HeI}}$ is estimated by Dubrovich & Grachev (2005) by assuming a similar form to that used for Λ_{nS+nD}^H :

$$\Lambda_{nS/nD}^{\text{HeI}} = \frac{1045 A^{\text{HeI}}}{g_{nS+nD}} \left(\frac{n-1}{n+1} \right)^{2n} \frac{11n^2 - 41}{n}, \quad (7)$$

where A^{HeI} is a fitting parameter (which is still uncertain both theoretically and experimentally). According to Dubrovich & Grachev (2005), reasonable values of A range from 10 to 12 s^{-1} , and we take $A = 11 \text{ s}^{-1}$ here. In our calculation, we include these extra two-photon rates up to $n=40$ for H and up to $n=10$ for HeI.

The other additional channel included is the spin-forbidden transition between the triplet 2^3P_1 and singlet 1^1S_0 states in HeI. This is an intercombination/semi-forbidden electric-dipole transition which emits a single photon and therefore we can calculate the corresponding net rate by using the bound-bound resonant rate expression, i.e.

$$\Delta R_{2^3P_1-1^1S_0} = p_{2^3P_1,1^1S_0} \times (n_{2^3P_1} R_{2^3P_1,1^1S_0} - n_{1^1S_0} R_{1^1S_0,2^3P_1}), \quad (8)$$

where

$$R_{2^3P_1,1^1S_0} = A_{2^3P_1,1^1S_0} + B_{2^3P_1,1^1S_0} \bar{J}, \quad (9)$$

$$R_{1^1S_0,2^3P_1} = B_{1^1S_0,2^3P_1} \bar{J}, \quad (10)$$

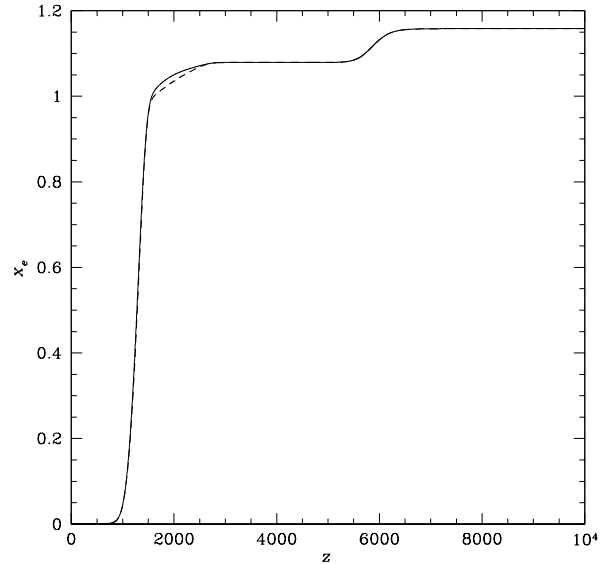


Figure 1. The ionization fraction x_e as a function of redshift z . The solid line is calculated using the original multi-level code of Seager, Sasselov & Scott (2000), while the dashed line includes all the extra forbidden transitions discussed here.

$$p_{2^3P_1,1^1S_0} = \frac{1 - e^{-\tau_s}}{\tau_s}, \quad \text{with} \quad (11)$$

$$\tau_s = \frac{A_{2^3P_1,1^1S_0} \lambda_{2^3P_1,1^1S_0}^3}{8\pi H(z)} \left[\frac{g_{2^3P_1} n_{1^1S_0} - n_{2^3P_1}}{g_{1^1S_0}} \right]. \quad (12)$$

Here $A_{2^3P_1,1^1S_0}$, $B_{2^3P_1,1^1S_0}$ and $B_{1^1S_0,2^3P_1}$ are the Einstein coefficients, $p_{2^3P_1,1^1S_0}$ is the Sobolev escape probability, τ_s is the Sobolev optical depth (see Seager, Sasselov & Scott 2000, and references therein), $\lambda_{2^3P_1,1^1S_0}$ is the wavelength of the energy difference between states 2^3P_1 and 1^1S_0 , and \bar{J} is the blackbody intensity with temperature T_R .

This $2^3P_1-1^1S_0$ transition is not the lowest transition between the singlet and the triplet states. The lowest one is the forbidden magnetic-dipole transition between 2^3S_1 and 1^1S_0 , with Einstein coefficient $A_{2^3S_1,1^1S_0} = 1.73 \times 10^{-4} \text{ s}^{-1}$ (Lin, Johnson & Dalgarno 1977). However, this is much smaller than $A_{2^3P_1,1^1S_0} = 177.58 \text{ s}^{-1}$ (Lach & Pachucki 2001; Drake & Morton, in preparation), so this transition can be neglected. Note that Dubrovich & Grachev (2005) used an older value of $A_{2^3P_1,1^1S_0} = 233 \text{ s}^{-1}$ (Lin, Johnson & Dalgarno 1977) in their calculation.

We use the Bader-Deuffhard semi-implicit numerical integration scheme (see Section 16.6 in Press et al. 1992) to solve the above rate equations. All the numerical results are carried out using the Λ CDM model with cosmological parameters: $\Omega_B = 0.04$; $\Omega_{\text{CDM}} = 0.2$; $\Omega_\Lambda = 0.76$; $\Omega_K = 0$; $Y_p = 0.24$; $T_0 = 2.725 \text{ K}$ and $h = 0.73$ (consistent with those in Spergel et al. 2006). Here Y_p is the primordial He abundance and T_0 the present background temperature.

3 RESULTS

3.1 Change in ionization fraction

The recombination histories calculated using the previous multi-level code (Seager, Sasselov & Scott 2000) and the

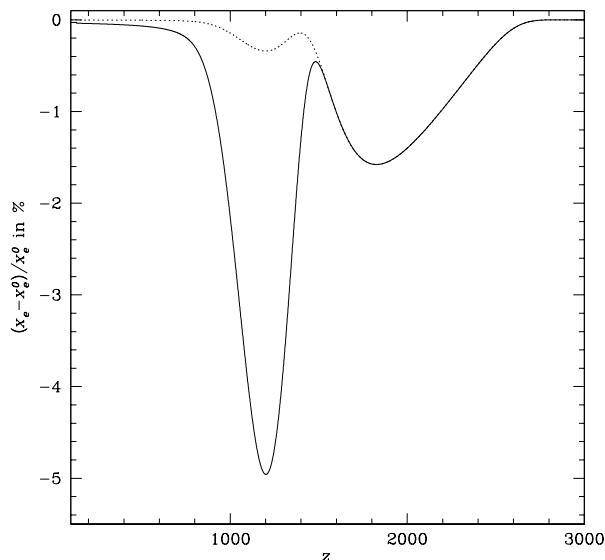


Figure 2. The fractional difference (‘new’ minus ‘old’) in x_e between the two models plotted in Fig. 1 as a function of redshift z . The solid and dotted lines are the models with the two-photon rates for H given by Dubrovich & Grachev (2005) and the scaled one given by equation (6), respectively. Both curves are calculated using all the HeI forbidden transitions as discussed in the text.

code in this paper are shown in Fig. 1, where $x_e \equiv n_e/n_H$ is the ionization fraction relative to hydrogen. As we have included more transitions in our model, and these give electrons more channels to cascade down to the ground state, we expect the overall recombination rate to speed up, and that this will be noticeable if the rates of the extra forbidden transitions are significant. From Fig. 1, we can see that the recombination to HeI is discernibly faster in the new calculation. Fig. 2 shows the difference in x_e with and without the extra forbidden transitions. The dip at around $z = 1800$ corresponds to the recombination of HeI and the one around $z = 1200$ is for H. Overall, the addition of the forbidden transitions claimed by Dubrovich & Grachev (2005) leads to greater than 1 per cent change in x_e over the redshift range where the CMB photons are last scattering.

In the last Section, we found that the approximated two-photon rate given by Dubrovich & Grachev (2005) for H with $n=3$ was overestimated by more than a factor of 10. By considering only this extra two-photon transition, the approximate rate gives more than a per cent difference in x_e , while with the more accurate numerical rates, the change in x_e is less than 0.1 per cent (as shown in Fig. 3). Based on this result, we do not need to include this two-photon transition, as it brings much less than a per cent effect on x_e . For estimating the effect of the extra two-photon transitions for higher n , we use the scaled two-photon rate given by equation (6). The result is plotted in Fig. 4. The change in x_e with the scaled two-photon rates is no more than 0.4 per cent, while the one with the Dubrovich & Grachev (2005) approximated rates brings about a 5 per cent change.

For HeI, Dubrovich & Grachev (2005) included the two-photon transitions from $n=6$ to 40, since they claimed that the approximate formula (equation 7) is good for $n > 6$. In our calculation, we use $\Lambda_{nS/nD}^{\text{HeI}}$ from the approximate formula for the two-photon transitions of $n=3$ to 10, since this is the best one can do for now (and the formula at least gives

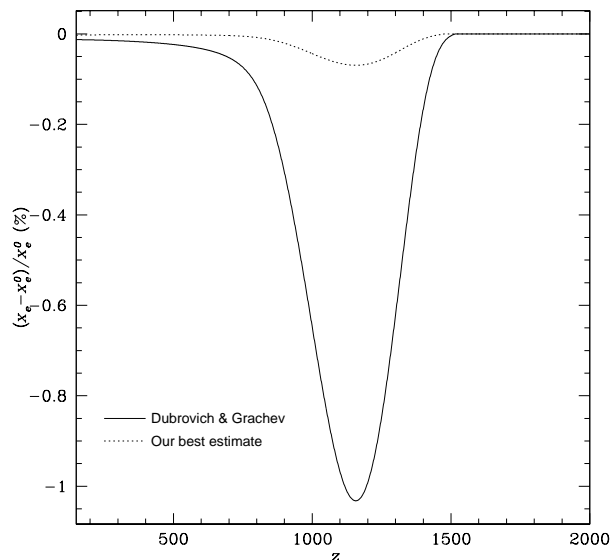


Figure 3. Fractional change in x_e with the addition of the two-photon transition from 3S and 3D to 1S for H. The solid line is calculated with the approximate rate given by Dubrovich & Grachev (2005) while the dashed line is calculated with the numerical rates given by Cresser et al. (1986).

the right order of magnitude). The addition of the singlet-triplet $2^3P_1-1^1S_0$ transition and the $n^1S_0-1^1S_0$ and $n^1D_2-1^1S_0$ two-photon transitions with $n=3-10$ cause more than 1 per cent changes in x_e (as shown in Fig. 2). The $2^3P_1-1^1S_0$ transition has the biggest effect on x_e .

Fig. 5 shows the fractional difference in x_e using different combinations of additional forbidden transitions. We can see that the $2^3P_1-1^1S_0$ transition alone causes more than a 1 per cent change in x_e , and the addition of each two-photon transition only gives about another 0.1 per cent change. The extra two-photon transitions from higher excited states (larger n) have a lower effect on x_e compared with that from small n , and we checked that this trend continues to higher n . However, the convergence is slow with increasing n . Therefore, one should also consider these two-photon transitions with $n > 10$ for HeI, and the precise result will require the use of accurate rates, rather than an approximate formula such as equation (7). For the $2^3P_1-1^1S_0$ transition, Dubrovich & Grachev (2005) adopted an older and slightly larger rate, and this causes a larger change of the ionization fraction (about 0.5 per cent more compared with that calculated with our best rate), as shown in Fig. 6.

3.2 The importance of the forbidden transitions

One might wonder why the semi-forbidden transitions are significant in recombination *at all*, since the spontaneous rate (or the Einstein A coefficient) of the semi-forbidden transitions are about 6 orders of magnitude (a factor of α^2 , where α is the fine-structure constant) smaller than those of the resonant transitions. Let us take HeI as an example for explaining the importance of the spin-forbidden $2^3P_1-1^1S_0$ transition in recombination. The spontaneous rate is equal to 177.58 s^{-1} for this semi-forbidden transition, which is much smaller than $1.7989 \times 10^9 \text{ s}^{-1}$ for the $2^1P_1-1^1S_0$ resonant transition. But when we calculate the net rate

Table 1. The percentage of electrons cascading down in each channel from $n = 2$ states to the 1^1S_0 ground state for He I.

	$2^1S_0 \rightarrow 1^1S_0$ (two-photon)	$2^1P_1 \rightarrow 1^1S_0$ (resonant)	$2^3P_1 \rightarrow 1^1S_0$ (spin-forbidden)
code from Seager, Sasselov & Scott (2000)	30.9%	69.1%	–
this work	17.3%	39.9%	42.8%

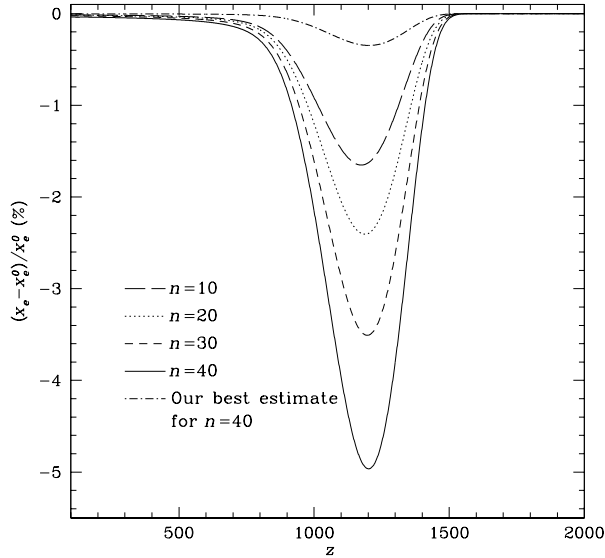


Figure 4. Fractional change in x_e with the addition of different forbidden transitions for H. The long-dashed, dotted, dashed and solid lines include the two-photon transitions up to $n = 10, 20, 30$ and 40 , respectively, using the approximation for the rates given by equation (5). The dot-dashed line is calculated with the scaled rate from equation (6).

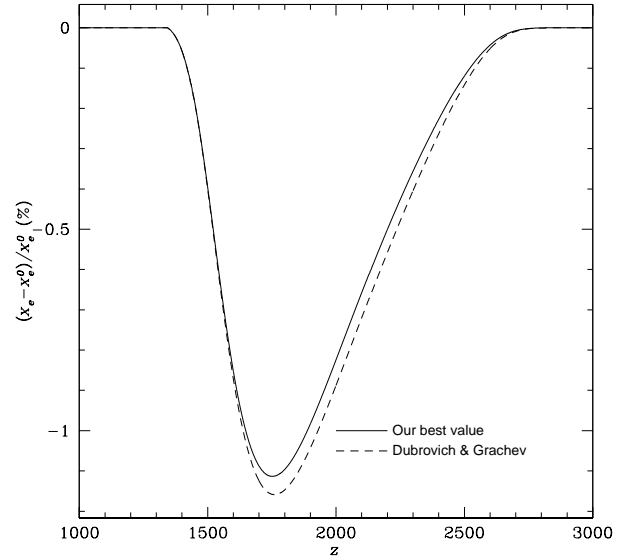


Figure 6. Fractional change in x_e with only the $2^3P_1-1^1S_0$ forbidden transition. The solid line is calculated with the rate $A = 233s^{-1}$ from Dubrovich & Grachev (2005) and the dashed line is computed with our best value $A = 177.58s^{-1}$ from Lach & Pachucki (2001).

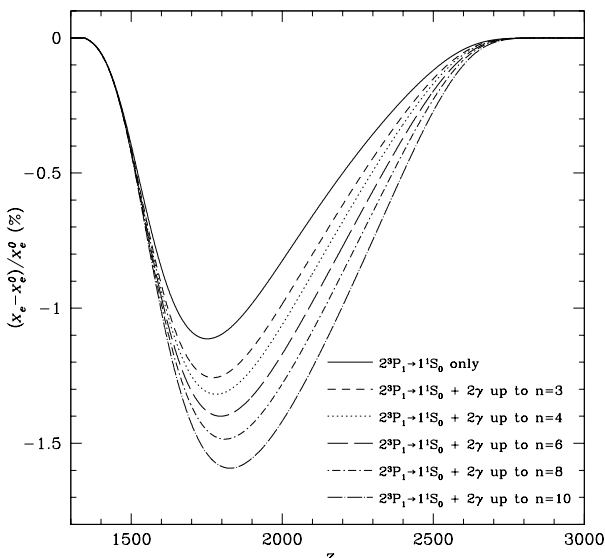


Figure 5. Fractional change in x_e with the addition of different forbidden transitions for He I as a function of redshift. The solid line corresponds to the calculation with only the $2^3P_1-1^1S_0$ spin-forbidden transition. The short-dashed, dotted, long-dashed, dot-dashed and long dot-dashed lines include both the spin-forbidden transition and the two-photon (2γ) transition(s) up to $n = 3, 4, 6, 8$ and 10 , respectively.

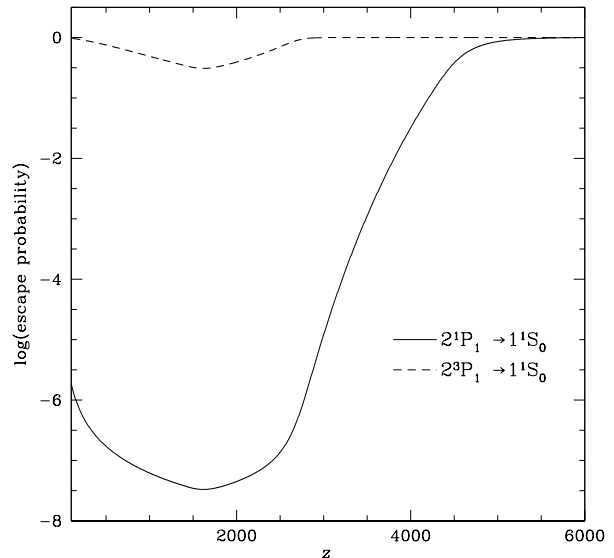


Figure 7. Escape probability p_{ij} as a function of redshift. The solid line corresponds to the resonant transition between 2^1P_1 and 1^1S_0 , while the dashed line refers to the spin-forbidden transition between 2^3P_1 and 1^1S_0 .

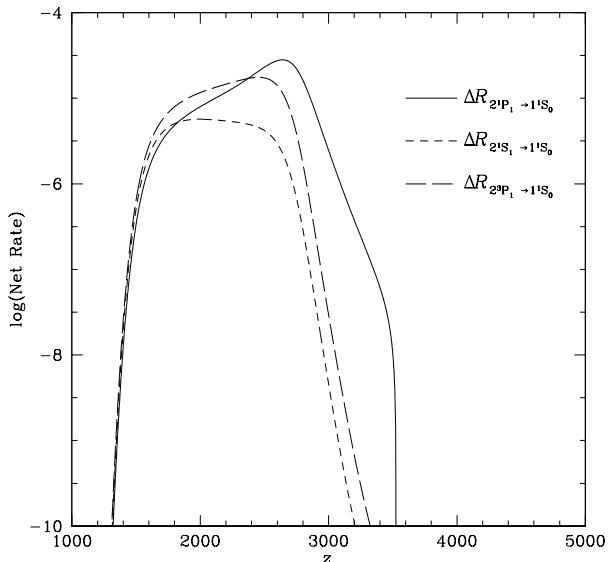


Figure 8. Net bound-bound rates for HeI as a function of redshift. The solid line is the resonant transition between 2^1P_1 and 1^1S_0 , the short-dashed line is the two-photon transition between 2^1S_1 and 1^1S_0 . And the long-dashed line is the spin-forbidden transition between 2^3P_1 and 1^1S_0 .

[see equation (8)], we also need to include the effect of absorption of the emitted photons by the surrounding neutral atoms, and we take this into account by multiplying the net bound-bound rate by the Sobolev escape probability p_{ij} (Seager, Sasselov & Scott 2000). If $p_{ij} = 1$, the emitted line photons can escape to infinity, while if $p_{ij} = 0$ the photons will all be reabsorbed and the line is optically thick. Fig. 7 shows that the escape probability of the $2^1P_1-1^1S_0$ resonant transition is about 7 orders of magnitude smaller than the spin-forbidden transition. This makes the two net rates roughly comparable, as shown in Fig. 8. From equation (11), we can see that the easier it is to emit a photon, the easier that photon can be re-absorbed, because the optical depth τ_s is directly proportional to the Einstein A coefficient. So when radiative effects dominate, it is actually natural to expect that some forbidden transitions might be important (although this is not true in a regime where collisional rates dominate which is often the case in astrophysics). In fact for today’s standard cosmological model, slightly more than half of all the hydrogen atoms in the Universe recombined via a forbidden transition (Wong, Seager & Scott 2006). Table 1 shows that this is also true for helium.

In the previous multi-level calculation (Seager, Sasselov & Scott 2000), there was no direct transition between the singlet and triplet states. The only communication between them was via the continuum, through the photo-ionization and photo-recombination transitions. Table 1 shows how many electrons cascade down through each channel from $n = 2$ states to the ground state. In the previous calculation, about 70% of the electrons went down through the $2^1P_1-1^1S_0$ resonant transition. In the new calculation, including the spin-forbidden transition between the triplets and singlets, there are approximately the same fraction of electrons going from the 2^1P_1 and 2^3P_1 states to the ground state (actually slightly more going from 2^3P_1 in the current cosmological model). This shows that we should certainly include this forbidden transition in

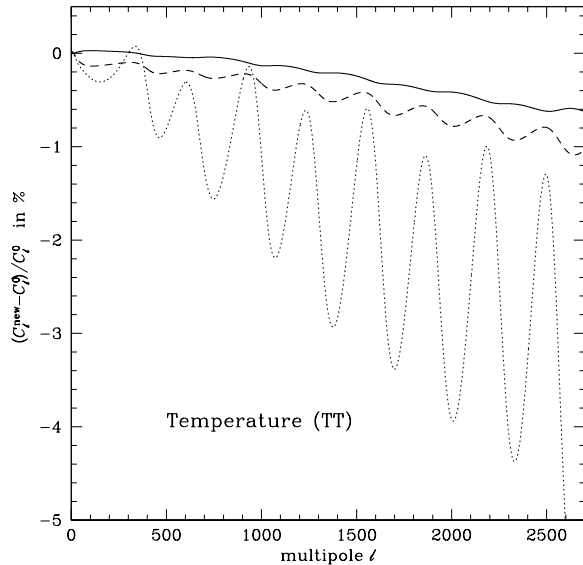


Figure 9. Relative change in the temperature (TT) angular power spectrum due to the addition of the forbidden transitions. The solid line includes the spin-forbidden transition and also the two-photon transitions up to $n = 10$ for HeI, the dotted line includes all the above transitions and also the two-photon transitions up to $n = 40$ for H calculated with the approximate rates given by Dubrovich & Grachev (2005). The dashed line is computed with the same forbidden transitions as the dotted line, but with our scaled rates (and represents our best current estimate).

future calculations. Our estimate is that only about 40% of helium atoms reach the ground state without going through a forbidden transition.

How about the effect of other forbidden transitions in HeI recombination? We have included all the semi-forbidden electric-dipole transitions with $n \leq 10$ and $\ell \leq 7$, and with oscillator strengths larger than 10^{-6} given by Drake & Morton (private communication). There is no significant change found in the ionization fraction. Besides the $2^3P_1-1^1S_0$ transition, all the other extra semi-forbidden transitions are among the higher excited states where the resonant transitions dominate. This is because these transition lines are optically thin and the escape probabilities are close to 1.

3.3 Effects on the anisotropy power spectrum

The CMB anisotropy power spectrum C_ℓ depends on the detailed profile of the evolution of the ionization fraction x_e . This determines the thickness of the photon last scattering surface, through the visibility function $g(z) \equiv e^{-\tau} d\tau/dz$, where τ is the Thomson scattering optical depth ($\tau = c \sigma_T \int n_e(dt/dz) dz$). The function $x_e(z)$ sets the epoch when the tight coupling between baryons and photons breaks down, i.e. when the photon diffusion length becomes long, and the visibility function fixes the time when the fluctuations are effectively frozen in (see Hu et al. 1995; Seager, Sasselov & Scott 2000, and references therein). The addition of the extra forbidden transitions speeds up both the recombination of H and He I, and hence we expect that there will be changes in C_ℓ .

In order to perform the required calculation, we have used the code CMBFAST (Seljak & Zaldarriaga 1996) and

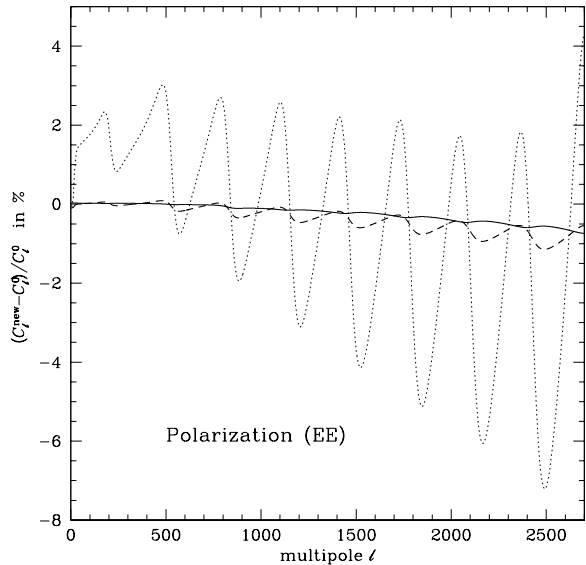


Figure 10. Relative change in the polarization (EE) angular power spectrum due to the addition of the forbidden transitions, with the curves the same as in Fig. 9.

modified it to allow the input of an arbitrary recombination history. Figs. 9 and 10 show the relative changes in the CMB temperature (TT) and polarization (EE) anisotropy spectra, respectively, with different combinations of extra forbidden transitions. The overall decrease of free electrons brings a suppression of C_ℓ over a wide range of ℓ .

For He I, there is less x_e at $z \simeq 1400 - 2500$, which leads to an earlier relaxation of tight coupling. Therefore, both the photon mean free path and the diffusion length are longer. Moreover, the decrease of x_e in the high- z tail results in increased damping, since the effective damping scale is an average over the visibility function. This larger damping scale leads to suppression of the high- ℓ part of the power spectrum. From Figs. 9 and 10, we can see a decrease of C_ℓ (for both TT and EE) toward high ℓ for He I, with the maximum change being about 0.6 percent.

For H, the change of C_ℓ is due to the decrease in x_e at $z \simeq 600 - 1400$ (see Fig. 2). There are two basic features in the curve of change in C_ℓ (the dotted and dashed lines in Fig. 9). Firstly, the power spectrum is suppressed with increasing ℓ , due to the lower x_e in the high- z tail ($z > 1000$). Secondly, there are a series of wiggles, showing that the locations of the acoustic peaks are slightly shifted. This is due to the change in the time of generation of the C_ℓ s in the low- z tail. C_ℓ^{EE} actually shows an increase for $\ell \leq 1000$ (see Fig. 10); this is caused by the shift of the center of the visibility function to higher z , leading to a longer diffusion length. Polarization occurs when the anisotropic hot and cold photons are scattered by the electrons. The hot and cold photons can interact with each other within the diffusion length, and therefore, a longer diffusion length allows more scatterings and leads to a higher intensity of polarization at large scales.

With the approximate rates used by Dubrovich & Grachev (2005), the maximum relative change of C_ℓ^{TT} is about 4 percent and for C_ℓ^{EE} it is about 6 percent. The overall change is thus more than 1 percent over a wide range of ℓ . However, if we adopt the scaled two-photon rate given by equation (6), the relative changes of C_ℓ^{TT} and C_ℓ^{EE} are no more than 1 per cent. Note

that we do not plot the temperature-polarization correlation power spectrum here, since there is no dramatically different change found (and relative differences are less meaningful since C_ℓ^{TE} oscillates around zero).

4 DISCUSSIONS

In our model we only consider the semi-forbidden transitions with $n \leq 10$ and $\ell \leq 7$ for He I and the two-photon transitions from the higher S and D states to the ground state for H and He I. It would be desirable to perform a more detailed investigation of all the other forbidden transitions, which may provide more paths for the electrons to cascade down to the ground state and speed up the recombination process. In this paper we have tried to focus on the forbidden transitions which are likely to be the most significant. However we caution that, if the approximations used are inadequate, or other transitions prove to be important, then our results will not be accurate.

There are several other approximations that we have adopted in order to perform our calculations. For example, we consider the *non-resonant* two-photon rates for higher excited states. The two-photon transitions from higher excited states ($n \geq 3$) to the ground state are more complicated than the 2S–1S transition, because of the resonant intermediate states. For example, for the 3S–1S two-photon transition, the spectral distribution of the emitted photons shows infinities (resonance peaks) at the frequencies corresponding to the 3S–2P and 2P–1S transitions (Tung et al. 1984). Here, we use only the non-resonant rates, by assuming a smooth spectral distribution of the emitted photons; this probably gives a lower limit on the change of x_e and C_ℓ coming from these extra forbidden transitions. The correct way to treat this would be to consider the rates and feedback from medium using the full spectral distribution of the photons and radiative transfer; this will have to wait for a future study.

Besides the consideration of more forbidden transitions, there are many other improvements that could be made to the recombination calculation. In particular, Rubino-Martin, Chluba & Sunyaev (2006) showed that a multi-level calculation of the recombination of H with the inclusion of separate ℓ -states can give more than 20 per cent difference in the population of some levels compared with the thermal equilibrium assumption for each n -shell. The latest calculation, considering up to 100 shells, is presented by Chluba, Rubino-Martin & Sunyaev (2006), but does not include all the forbidden transitions studied here. A more complete calculation should be done by combining the forbidden transitions in a code with full angular momentum states, and we leave this to a future study. There are also other elaborations which could be included in future calculations, which we now describe briefly.

The rate equation we use for all the two-photon transitions only includes the spontaneous term, assuming there is no interaction with the radiation background (see equation (3)). Chluba & Sunyaev (2006) suggested that one should also consider the stimulated effect of the 2S–1S two-photon transition for H, due to photons in the low frequency tail of the CMB blackbody spectrum. Leung, Chan & Chu (2004) additionally argued that the change of the adiabatic

index of the matter should also be included, arising due to the neutralization of the ionized gas. These two modifications have been studied only in an effective three-level atom model, and more than a percent change in x_e was claimed in each case (but see Wong & Scott (2006) for arguments against the effect claimed by Leung et al. 2004).

For the background radiation field \bar{J} , we approximated it with a perfect blackbody Planck spectrum. This approximation is not completely correct for the recombination of H, since the He line distortion photons redshift into a frequency range that can in principle photo-ionize the neutral H (Dell’Antonio & Rybicki 1993; Seager, Sasselov & Scott 2000; Wong, Seager & Scott 2006). Although we expect this secondary distortion effect to bring the smallest change on x_e among all the modifications suggested here, it is nevertheless important to carry out the calculation self-consistently, particularly for the spectral line distortions. In order to obtain an accurate recombination history, we therefore need to perform a full multi-level calculation with separate ℓ -states and all the improvements suggested above, which we plan to do in a later paper.

For completeness we also point out that the accuracy of the physical constants is important for recombination as well. The most uncertain physical quantity in the recombination calculation is the gravitational constant G . The value of G used previously in the RECFAST code is $6.67259 \times 10^{-11} \text{m}^3 \text{kg}^{-1} \text{s}^{-2}$ and the latest value (e.g. from the Particle Data Group, Yao et al. 2006) is $6.6742 \times 10^{-11} \text{m}^3 \text{kg}^{-1} \text{s}^{-2}$. Another quantity we need to modify is the atomic mass ratio of ^4He and ^1H , $m_{^4\text{He}}/m_{^1\text{H}}$, which was previously taken to be equal to 4 (as pointed out by Steigman 2006). By using the atomic masses given by Yao et al. (2006), the mass ratio is equal to 3.9715. The overall change in x_e is no more than 0.1 per cent after updating these two constants in both RECFAST and multi-level code.

5 CONCLUSIONS

In this paper, we have computed the cosmological recombination history by using a multi-level code with the addition of the 2^3P_1 to 1^1S_0 spin-forbidden transition for HeI and the two-photon transitions from $n\text{S}$ and $n\text{D}$ states to the ground state for both H and HeI. With the approximate rates from Dubrovich & Grachev (2005), we find that there is more than a per cent decrease in the ionization fraction, which agrees broadly with the result they claimed. However, the only available accurate numerical value of two-photon rate with $n \geq 3$ is for the 3S to 1S and 3D to 1S transitions for H. We found that the approximate rates from Dubrovich & Grachev (2005) were overestimated, and instead we considered a scaled rate in order to agree with the numerical $n = 3$ two-photon rate. With this scaled rate, the change in x_e is no more than 0.5 per cent.

Including these extra forbidden transitions, the change in the CMB anisotropy power spectrum is more than 1 per cent, which will potentially affect the determination of cosmological parameters in future CMB experiments. Since one would like the level of theoretical uncertainty to be negligible, it is essential to include these forbidden transitions in the recombination calculation. In addition, we still re-

quire accurate spontaneous rates to be calculated for the two-photon transitions and also a code which includes at least all the modifications suggested in Section 4, in order to obtain the $C_\ell\text{s}$ down to the 1 per cent level. Achieving sub-percent accuracy in the calculations is challenging!

However, the stakes are high – the determination of the parameters which describe the entire Universe – and so further work will be necessary. Systematic deviations of the sort we have shown would potentially lead to incorrect values for the spectral tilt derived from Planck and even more ambitious future CMB experiments, and hence incorrect inferences about the physics which produced the density perturbations in the very early Universe. It is amusing that in order to understand physics at the 10^{15} GeV energy scale we need to understand eV scale physics in exquisite detail!

6 ACKNOWLEDGEMENTS

This work would have been impossible without the earlier discussions with Sara Seager. We thank Donald C. Morton for useful conversations and providing us with updated forbidden transition rates. We are grateful to Peter J. Storey for providing the data for the photo-ionization cross-section of neutral helium. We would also like to thank Alexander Dalgarno, Victor K. Dubrovich, Christopher Hirata and Eric Switzer for useful discussions. This work made use of the code CMBFAST, written by Uros Seljak and Matias Zaldarriaga. This research was supported by the Natural Sciences and Engineering Research Council of Canada and a University of British Columbia Graduate Fellowship.

REFERENCES

- Bauman R.P., Porter R.L., Ferland G.J., MacAdam K.B., 2005, *ApJ*, 628, 541
- Chluba J., Sunyaev R.A., 2006, *A&A*, 446, 39
- Chluba J., Rubino-Martin J.A., Sunyaev R.A., 2006, *astro-ph/0608242*
- Cresser J.D., Tang A.Z., Salamo G.J., Chan F.T., 1986, *Phys. Rev. A*, 33, 3, 1677
- Dell’Antonio I.P., Rybicki G.B., 1993, in *ASP Conf. Ser.* 51, *Observational Cosmology*, ed. G. Chincarini et al. (San Francisco:ASP), 548
- Drake G.W.F., Morton D.C., 2006, in preparation for the *Astrophysical Journal*
- Dubrovich V.K., Grachev S.I., 2005, *Astronomy Letters*, 31, 6, 35
- Florescu V., Patrascu S., Stoican O., 1987, *Phys. Rev. A*, 36, 2155
- Florescu V., Schneider I., Mihailescu I.N., 1988, *Phys. Rev. A*, 38, 4, 2189
- Goldman S.P., 1989, *Phys. Rev. A*, 40, 1185
- Hu W., Scott D., Sugiyama N., White M., 1995, *Phys. Rev. D*, 52, 5498
- Hummer D.G., Storey P.J., 1998, *MNRAS*, 297, 1073
- Labzowsky L.N., Shonin A.V., Soloviyev D.A., 2005, *Journal of Physics B*, 38, 265
- Lach G., Pachucki K., 2001, *Phys. Rev. A*, 64, 042510
- Leung P.K., Chan C.W., Chu M.C., 2004, *MNRAS*, 349, 2, 632

- Lewis A., Weller J., Battye R., 2006, astro-ph/0606552
Lin C.D., Johnson W.R., Dalgarno A., 1977, Phys. Rev. A, 15, 1, 154
Morton D.C., Wu Q., Drake G.W.F., 2006, Can. J. Phys., 84, 83
Peebles P.J.E. 1968, ApJ, 153, 1
Planck, 2006, ESA-SCI(2005)1
Press W.H., Flannery B.P., Teukolsky S.A., Vetterling W.T., 1992, Numerical Recipes in C: The Art of Scientific Computing, Cambridge Univ. Press, Cambridge, UK
Rubino-Martin J.A., Chluba J., Sunyaev R.A., 2006, astro-ph/0607373
Santos J.P., Parente F., Indelicato P., 1998, Eur. Phys. J., D3, 43
Seager S., Sasselov D.D., Scott D., 1999, ApJ, 523, L1
Seager S., Sasselov D.D., Scott D., 2000, ApJS, 128, 407
Seljak U., Sugiyama N., White M., Zaldarriaga M., 2003, Phys. Rev. D, 68, 083507
Seljak U., Zaldarriaga M., 1996, ApJ, 463, 1
Spergel D.N., et al., 2006, astro-ph/0603449
Steigman G., 2006, astro-ph/0606206
Storey P.J., Hummer D.G., 1991, Comput. Phys. Commun., 66, 12
Tung J.H., Ye X.M., Salamo G.J., Chan F.T., 1984, Phys. Rev. A, 30, 1175
Yao W.-M. et al., 2006, Journal of Physics G, 33, 1
Wong W.Y., Seager S., Scott D., 2006, MNRAS, 367, 1666
Wong W.Y., Scott D., 2006, astro-ph/0612322
Zel'dovich Y.B., Kurt V.G., Sunyaev R.A., 1968, Zh. Eksp. Teor. Fiz., 55, 278; English transl., 1969, Soviet Phys. JETP Lett., 28, 146

This paper has been typeset from a \TeX / \LaTeX file prepared by the author.